IL NUOVO CIMENTO **48 C** (2025) 242
DOI 10.1393/ncc/i2025-25242-7

COMMUNICATIONS: SIF Congress 2024

Preliminary evaluation of calibration method on Double Crystal Monochromator and Time-of-Flight Bragg Edge Neutron Transmission analysis

M. MARABOTTO(1)(2), A. RE(3)(2), L. GUIDORZI(3)(2), A. LO GIUDICE(3)(2), S. GRASSINI(4)(2), F. GRAZZI(5)(6), F. CANTINI(7)(6), L. GIUNTINI(7)(6), G. MARCUCCI(8)(9), A. SCHERILLO(9), R. RAMADHAN(9), M. BUSI(10), C. B. LARSEN(10), S. SAMOTHRAKITIS(10) and D. DI MARTINO(8)

(1) *Dipartimento di Elettronica e Telecomunicazioni, Politecnico di Torino - Torino, Italy*
(2) *INFN, Sezione di Torino - Torino, Italy*
(3) *Dipartimento di Fisica, Università di Torino - Torino, Italy*
(4) *Dipartimento di Scienza Applicata e Tecnologia, Politecnico di Torino - Torino, Italy*
(5) *CNR, Istituto di Fisica Applicata Nello Carrara - Firenze, Italy*
(6) *INFN, Sezione di Firenze - Firenze, Italy*
(7) *Dipartimento di Fisica, Università di Firenze - Firenze, Italy*
(8) *Dipartimento di Fisica, Università degli Studi di Milano-Bicocca and INFN, Sezione di Milano-Bicocca - Milano, Italy*
(9) *Science and Technology Facilities Council, ISIS Neutron and Muon Source - Didcot, UK*
(10) *Laboratory for Neutron Scattering and Imaging, PSI - Villigen, Switzerland*

received 31 January 2025

Summary. — Ancient metallurgy is crucial for understanding the artistic and technological evolution of past civilisations. Neutron-based techniques offer a non-invasive approach to determine alloy and phase composition of ancient artefacts. The work presented here is part of the INFN CHNet_BRONZE project, aiming to quantitatively calibrate neutron techniques for the analysis of Cu-based archaeological items. It focuses on the preliminary wavelength calibration of the measurements carried out with the Bragg-Edge Neutron Transmission (BENT) technique, a non-invasive method that reveals composition, texture and microstructure of materials over large areas of the samples, exploiting 2D imaging detectors.

1. – Introduction

Ancient metallurgy, in particular of bronze and copper alloys, is a research topic of great relevance in the study of the artistic and technological evolution of past civilizations [1].

Neutron-based techniques can provide the alloy and phase composition of ancient artworks, revealing information on technological, degradation and conservation issues [2-4] while preserving the samples, a crucial aspect in Heritage Science. Moreover, the great penetration power of neutrons in materials of high atomic number and/or density as

well as their ability to provide good contrast between elements with close atomic weight and between isotopes give neutron-based techniques the potential to become one of the preferable techniques for the diagnosis of bronze artefacts. The INFN CHNet_BRONZE project aims at further developing non-invasive techniques based on neutron absorption and scattering for quantitative analysis of archaeological copper alloy items.

The work presented here is part of the project, concerning the neutron wavelength calibration procedure for the data acquired using the Bragg Edge Neutron Transmission (BENT) technique at two different neutron facilities, SINQ (PSI, Switzerland) and ISIS Neutron and Muon source (STFC, UK). Two different acquisition methods have been used, wavelength scan using a Double Crystal Monochromator (DCM) and Time-of-Flight (ToF), for which two different calibration approaches are needed.

2. – Method

BENT is performed measuring the neutron transmission across a sample at different wavelengths. The resulting spectrum shows a characteristic stepped pattern, the Bragg edges. From the analysis of the position, height, broadening of the edges and the shape of the curve, it is possible to obtain information on the composition, strain, texture and microstructure of the sample [5, 6].

BENT data has been acquired using the BOA instrument at PSI [7] and the IMAT beamline at ISIS [8].

A wavelength scan by means of a Double Crystal Monochromator (DCM) has been performed at BOA. In this case, multiple neutron radiographs are acquired selecting different wavelengths with the DCM in the desired range, (2.5−6.1) Å. The detection system consists of a LiF scintillator coupled with a CCD camera, with a field of view of 100×100 mm^2 and a pixel size of 48.8 μm. A schematic of the setup is shown in fig. 1(a).

At IMAT, the ToF approach has been used: it consists in measuring the transmission of a polichromatic neutron beam using a n-GEM detector capable of measuring, for each pixel, the arrival of neutrons and their time of flight. The ToF, given by the neutron time of flight t plus a time offset t_0 of the data processing electronics, is related to the wavelength λ according to

$$\lambda = \frac{h}{m}\frac{(t+t_0)}{L}, \tag{1}$$

where h is the Planck constant, m is the neutron mass and L is the neutron flight path.

The field of view is 100×100 mm^2, while the pixel size is 800 μm, therefore the spatial resolution is much lower with respect to the one available at PSI. The setup is schematized in fig. 1(b). The two different acquisition methods lead to distinct data

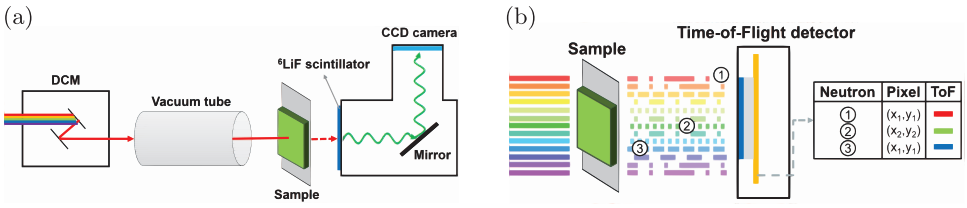

Fig. 1. – Schematic setups used at the two facilities. (a) PSI experiment, (b) ISIS experiment.

correction and processing. In particular, the neutron wavelength calibration procedure in the two cases is presented in sect. **3**.

3. – Wavelength calibration

Calibrating the neutron wavelengths for a BENT experiment is essential to ensure reliable and precise results. The calibration procedure for the DCM and ToF acquisition differs, since the data collected vary significantly between the two methods. However, in both cases a known calibrant is used, in this case α-iron powder for its high coherent cross-section and well separated Bragg edges.

3˙1. *Wavelength scan with DCM*. – The use of the monochromator, whose structure and functioning can be found in [7], allows to select specific wavelengths, but it induces a horizontal dispersion across the field of view (fig. 2(a)), caused by the divergence of the neutron beam entering the DCM. To correct this effect, the (110) Bragg edge position of the α-Fe, the most intense, is obtained for each column of pixels by fitting the derivative of the spectrum with a Gaussian model. The horizontal shift is then calculated as the difference from the position of the edge in the central column (fig. 2(b)). By a linear fit of the shift, an array of correction to subtract from the edge λ values measured on the samples can be obtained.

In this case, the measured dispersion of the wavelength across the FOV is $(7.955 \pm 0.013) \cdot 10^{-2}$ Å. Despite the much higher spatial resolution obtained with this method, the wavelength resolution, resulting from the resolution of the DCM itself ($\Delta\lambda/\lambda = 10\%$) and the wavelength dispersion effect, does not allow to perform fine analyses on alloys with similar compositions or strain measurements, as the required resolution for these kind of analyses is much higher [5].

3˙2. *ToF calibration*. – When performing a ToF experiment, the neutron wavelengths can be derived using eq. (1). However, the detector on IMAT is not fixed. This leads to a small uncertainty in its position, an thus in the L value. For this reason, the flight path is determined experimentally using the calibrant powder. In particular, the ToF of the Bragg edges for different lattice planes (hkl) of the α-Fe (spectrum reported in fig. 3(a)) are derived from the fit of the edges (the uncertainty of the obtained ToF values is below $2{\cdot}10^{-5}$ s). The nominal values of the Fe powder Bragg edges wavelengths are known using nxsPlotter [9] and a calibration curve can be obtained from the linear regression of

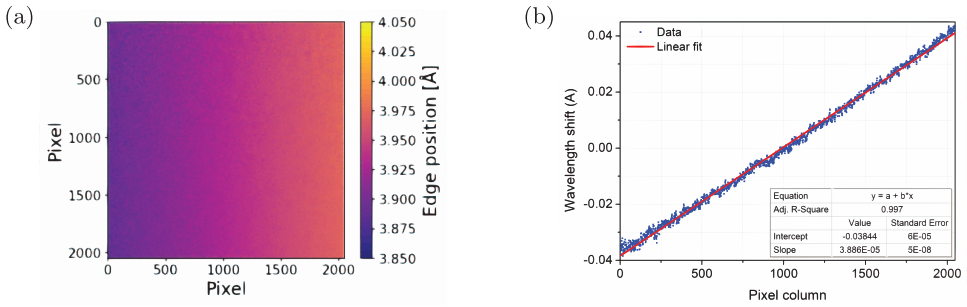

Fig. 2. – Wavelength dispersion correction. (a) Colormap of the (110) edge position in each pixel of the CCD camera. A horizontal gradient can be observed. (b) Linear fit of the shift of λ from the central value for each pixel column. The table reports the fitting parameters values and errors.

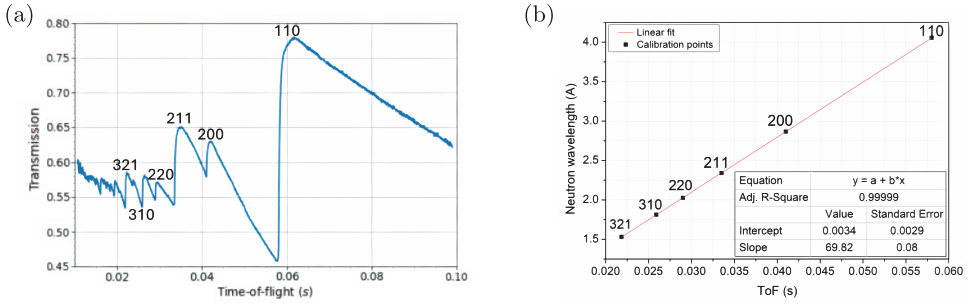

Fig. 3. – ToF calibration procedure. (a) Fe powder spectrum acquired on IMAT. Indexes for the different lattice planes (hkl) are indicated for the evaluated edges. (b) Linear regression of calibration points. Fitting parameters with uncertainties are reported in the table.

the calibration points, as shown in fig. 3(b). From the fitting parameters it is possible to calculate the flight path $L = 56.67 \pm 0.06$ m and the time offset $t_0 = (4.9 \pm 4.2) \cdot 10^{-5}$ s using eq. (1). These values are then used to derive the neutron wavelengths from the time-of-flight values, with a relative uncertainty less than 0.5%.

4. – Conclusions

When performing the Bragg Edge Neutron Transmission analysis, an accurate calibration of the neutron wavelengths is crucial to ensure good results. In this work, the horizontal wavelength dispersion along the FOV induced by the DCM is shown. In this case, the difference between the λ on the right and the left side of the FOV is $(7.955 \pm 0.013) \cdot 10^{-2}$ Å. The calibration procedure for ToF acquisitions is described, allowing to determine the instrumental time offset and the neutron flight path, $L = 56.67 \pm 0.06$ m, necessary to obtain the neutron wavelengths from the measured ToF.

* * *

We acknowledge the INFN (CSN 5) and the CNR within CNR-STFC Agreement 2021–2027 (N 0065606) for financial support. This work is based on experiments performed at SINQ, Paul Scherrer Institute (P20230414, P20240362) and at the ISIS Neutron and Muon Source, Science and Technology Facilities Council (RB2310722 [10]). We acknowledge Markus Strobl (PSI) and Winfried Kockelmann (ISIS) for support.

REFERENCES

[1] Roberts B. W. and Thornton C. P., *Archaeometallurgy in Global Perspective* (Springer, New York) 2014.
[2] Grazzi F. *et al.*, *Mater. Charact.*, **144** (2018) 387.
[3] Marcucci G. *et al.*, *Eur. Phys. J. Plus*, **139** (2024) 475.
[4] Depalmas A. *et al.*, *Archaeol. Anthropol. Sci.*, **13** (2021) 101.
[5] Sato H. *et al.*, *ISIJ Int.*, **61** (2021) 1584.
[6] Sato H. *et al.*, *Mater. Res. Proc.*, **15** (2020) 214.
[7] Morgano M. *et al.*, *Nucl. Instrum. Methods Phys. Res. Sect. A*, **754** (2014) 46.
[8] Kockelmann W. *et al.*, *J. Imaging*, **4** (2018) 47.
[9] Boin M., *J. Appl. Crystallogr.*, **45** (2012) 603.
[10] Re A. *et al.*, `https://doi.org/10.5286/ISIS.E.RB2310722` (2024).